

Dynamic study of dipole-dipole interaction effects in a magnetic nanoparticle system

T. Jonsson, P. Nordblad, and P. Svedlindh

Department of Materials Science, Uppsala University, Box 534, S-751 21 Uppsala, Sweden

(Received 1 July 1997; revised manuscript received 19 August 1997)

The effects of a dipole-dipole interaction on the magnetic relaxation in a magnetic nanoparticle system have been investigated using ac-susceptibility, magnetic relaxation, and magnetic noise measurements, which altogether cover a time window of nine decades. In the experimental time window, it is possible to distinguish two temperature regimes: a low-temperature regime where collective dynamics is probed, as evidenced by the appearance of magnetic aging and a significantly broadened magnetic relaxation, and a high-temperature regime where the magnetic relaxation is best described as single-particle dynamics. Moreover, the magnetic relaxation of the interacting particle system is shifted towards longer time scales, but gradually, at high temperatures, the relaxation rate approaches the rate of the noninteracting sample. [S0163-1829(98)05501-5]

I. INTRODUCTION

During the last couple of decades, spin glasses¹ (SG's) and diluted antiferromagnets² have been the favorite systems when investigating how disorder affects the properties of magnetic systems. It is only lately that frozen ferrofluids, i.e., ensembles of nanosized magnetic particles dispersed in different carrier liquids, have been used as experimental model systems for random magnets. A distinct advantage of using frozen ferrofluids is that the strength of the magnetic interaction easily can be tuned by controlling the concentration of magnetic particles in the ferrofluid.

The direction of the magnetic moment in a monodomain ferromagnetic particle is determined by the magnetic potential, which for a noninteracting magnetic particle is formed by the magnetic anisotropy and magnetic field energies. At finite temperatures, thermal fluctuations will enable the magnetic moment to point along other directions than the directions corresponding to the energy minima of the magnetic potential. Depending on the constraints set by the energies involved it is possible to derive more or less simple approximate expressions for the magnetic relaxation of noninteracting nanosized magnetic systems.³⁻⁵ Several experimental studies on such systems support the now existing models describing the dynamics.⁶⁻⁸

A nontrivial problem appears when the dipole fields due to neighboring magnetic particles become of importance, i.e., when the magnetic interaction energy becomes of the same order of magnitude as the other energies involved. If the particles are randomly distributed with their anisotropy axes pointing in arbitrary directions, the problem turns into an analytically unsolvable many-body problem. During the latest years, several studies of interaction effects in nanosized magnetic particle systems have been performed using different experimental methods,⁹⁻¹⁷ and in most cases the results have been interpreted within different mean-field-like models. In one investigation, though, the critical behavior close to the expected phase transition temperature was investigated and the results indicate that ingredients such as randomness and frustrated interactions in a magnetic particle system yield a super-spin-glass phase at low temperatures.¹⁷ To seek further understanding of the interaction effects in particle systems also computer simulation is an important tool,

whose main advantage is the easy way by which it is possible to tune parameters such as the relative strength of the anisotropy and interaction energies.¹⁸⁻²⁰

In this paper ac-susceptibility, magnetic noise, and magnetic relaxation measurements have been used to probe the dynamics of a nanosized magnetic particle system. The effects of the interaction are scrutinized by studying the change in the magnetic relaxation going from a noninteracting system to a system with a sizable interparticle interaction. The structure of the paper is as follows: In Sec. II some experimental details are described; in Sec. III the results are presented, while a more complete discussion of the results is presented in Sec. IV. The main conclusions of the experimental study are given in Sec. V.

II. EXPERIMENT

The experiments were performed on a sample consisting of nanosized maghemite, γ -Fe₂O₃, particles dispersed in hydrocarbon oil. The concentration by volume of particles was $\epsilon = 17\%$. This sample has been reported¹⁵ to exhibit spin-glass-like dynamics, such as aging, at low temperatures. An experimental study⁸ on a sample taken from the same batch of ferrofluid but having a volume concentration of $\epsilon = 0.03\%$ showed that the particle size distribution is well described by a γ distribution having an average particle diameter of $d_{av} = 80 \text{ \AA}$. The magnetic anisotropy constant was determined to be $K = 13.4 \text{ kJ/m}^3$,⁸ which implies that the average energy barrier, in the absence of a dipole-dipole interaction, is $E_{b,av} = 260 \text{ K}$. Since the carrier oil is an electrical insulator and since the particles are coated with a surfactant layer preventing the particles from being in direct contact with each other, it can be concluded that the magnetic interaction is of dipole-dipole type. The magnitude of this energy, corresponding to the interaction energy between two neighboring particles, can be estimated from $E_{d-d,av} = (\mu_0/24k_B)M_s^2d_{av}^3\epsilon$. Using the low-temperature value of the saturation magnetization, $M_s = 4.2 \times 10^5 \text{ A/m}$, this gives $E_{d-d,av} = 60 \text{ K}$ for the $\epsilon = 17\%$ sample. Below 180 K the hydrocarbon oil freezes and the particles become fixed randomly in space. All results presented below correspond to this temperature range.

In case of a noninteracting magnetic nanoparticle system,

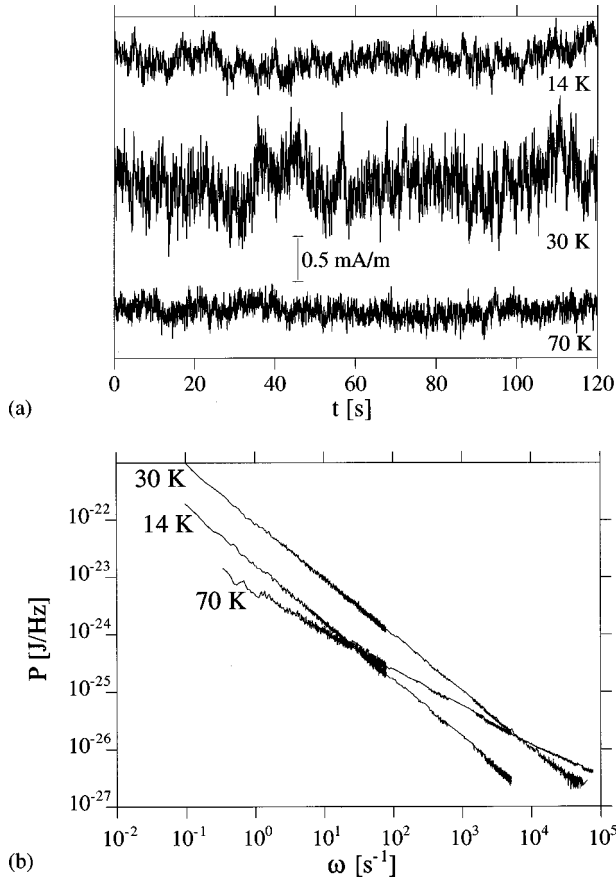


FIG. 1. (a) Magnetic noise as a function of time for the interacting γ - Fe_2O_3 sample. The different curves correspond to time traces taken at the temperatures 14 K, 30 K, and 70 K. (b) Averaged noise power spectra for the interacting γ - Fe_2O_3 sample. The different curves correspond to the temperatures 14 K, 30 K, and 70 K.

a simple Néel theory can be used to determine the distribution of energy barriers.^{6,8} A considerable part of the energy barrier distribution can be obtained by using only a limited experimental time window in the relaxation experiment by simply changing the temperature and hence the probed energy scale according to $E_b/k_B = T \ln(t_{\text{obs}}/\tau_0)$. This simple scaling relation cannot be used to analyze the energy barrier distribution for an interacting particle system since, as is the case also for spin glasses, no simple scaling law connecting time and temperature to a characteristic energy scale can be obtained. Instead, one has to measure the magnetic relaxation in an experimental time window as wide as possible to find out the essential features of the magnetic dynamics in an interacting particle system.

Two different experimental setups have been used: (i) A commercial ac susceptometer²¹ was used to measure the in-phase and out-of-phase components of the ac susceptibility. A cylindrical container, having a length of 15 mm and a diameter of 4 mm, was used as sample cup. The frequency was varied in the range 15 Hz–10 kHz, corresponding to an experimental time window of 1.6×10^{-5} – 10^{-2} s. (ii) A non-commercial low-field superconducting quantum interference device (SQUID) magnetometer operating in the time window 10^{-5} – 10^4 s. The sample was placed in a cylindrical container made of sapphire, having a length of 5 mm and a diameter of 1.5 mm, which was connected to a sapphire rod being in direct thermal contact with the thermometer and a

manganin heater. The details of the magnetometer are described elsewhere.²²

To cover the time window 10^{-5} – 10^4 s, it was necessary to make use of two different measurement techniques. Magnetic noise measurements cover observation times ranging from 10^{-5} to 10^1 s and zero-field-cooled (ZFC) magnetic relaxation measurements the time window 10^{-1} – 10^4 s. In the magnetic relaxation experiment, the sample is cooled in zero field from a high temperature where the sample displays a superparamagneticlike behavior. For this sample, 130 K was high enough to yield a superparamagnetic response. When reaching the measurement temperature, the sample is equilibrated a waiting time t_w before a small magnetic field is applied and the magnetization is recorded vs observation time t_{obs} . To simplify the analysis, it is important to use a small enough probing field h , so that the sample is probed in the linear response regime (this requirement should be fulfilled for all temperatures and time scales used in the experiments). In our experiments, $h = 1$ G was low enough to yield a linear response.

Measurements of the magnetic noise power spectral density $P(\omega)$ of the sample in the absence of applied fields were performed at different temperatures by connecting the output of the SQUID electronics to an HP 35670A dynamic signal analyzer. The noise was measured in three overlapping frequency intervals: (i) 0.01–12.5 Hz, (ii) 0.5–800 Hz, and (iii) 16 Hz–10 kHz. The number of spectra used for averaging varied between the three intervals: Interval (i) used 300, interval (ii) 2000, and interval (iii) 10 000 spectra. All averaged spectra were corrected for the background noise spectrum of the experimental setup. For temperatures where the magnetic noise due to the sample at high frequencies is of the same order or smaller than the background noise of the experimental setup, frequencies higher than typically 1 kHz were not used in the analysis.

The results from the different measurements can be inter-related using simple relations. The fluctuation-dissipation theorem²³ relates the magnetic noise power and the out-of-phase component of the ac susceptibility according to

$$P(\omega) = 2k_B T \frac{\chi''(\omega)}{\omega}. \quad (1)$$

Furthermore, the time-dependent magnetization $m(t_{\text{obs}})$ in a sample displaying a logarithmically slow relaxation is connected to the out-of-phase component of the ac susceptibility through the relation²⁴

$$S(t_{\text{obs}}) = 1/h \frac{\partial m(t_{\text{obs}})}{\partial \ln(t)} \approx \frac{2}{\pi} \chi''(\omega), \quad (2)$$

with $t_{\text{obs}} \approx 1/\omega$. It is convenient to analyze the experimental results in terms of the relaxation rate $S(t_{\text{obs}})$, since this quantity mirrors the relaxation time distribution in a straightforward manner.^{8,24}

III. RESULTS

A. Noise results

In Fig. 1(a), typical time traces of the SQUID output signal are plotted for the temperatures 14 K, 30 K, and 70 K.

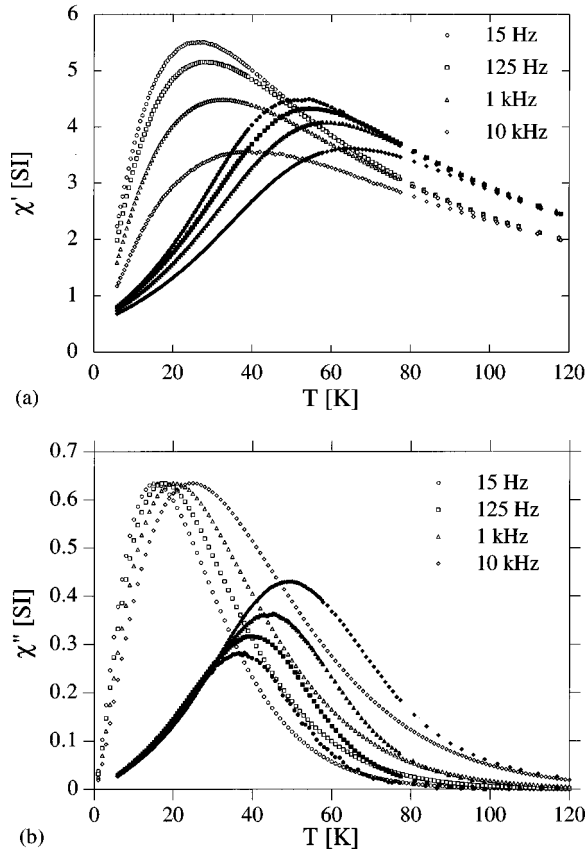


FIG. 2. χ vs T at different frequencies ranging from 15 Hz to 10 kHz for the noninteracting (open symbols) and the interacting (solid symbols) γ - Fe_2O_3 samples. (a) $\chi'(T)$ and (b) $\chi''(T)$.

The averaged noise power spectra for these temperatures are displayed in Fig. 1(b). These figures indicate that the noise power spectra at the two lower temperatures have a frequency dependence essentially following a $1/\omega$ dependence, which is similar to that found in spin glasses at low temperatures.²⁵ The high-temperature behavior, here represented by the results obtained at 70 K, is, however, different from the high-temperature behavior of spin glasses, where at temperatures above the spin glass temperature the noise power spectra show plateaus in the low-frequency limit. In the presently investigated particle system, the noise power spectra at high temperatures follow a $1/\omega^x$ dependence, with x taking values in the range 0.6–0.8.

One advantage of using results obtained from magnetic noise measurements is that these will not be influenced by demagnetization effects, which in case of heterogeneous magnetic materials may be difficult to compensate for.²⁶ Moreover, it may be that the shape of the ferrofluid changes while going from the liquid to the solid state. However, by comparing magnetic noise results with the field-probed ac-susceptibility and ZFC magnetic relaxation results an estimate of the effective demagnetization factor can be obtained. For all temperatures and time scales used in the present experimental study, a good conformity between the different results is achieved using the demagnetization factor $N=0.04$. For a comparison, this value is about 3 times smaller than the value suggested by the geometrical shape of the sapphire sample container.

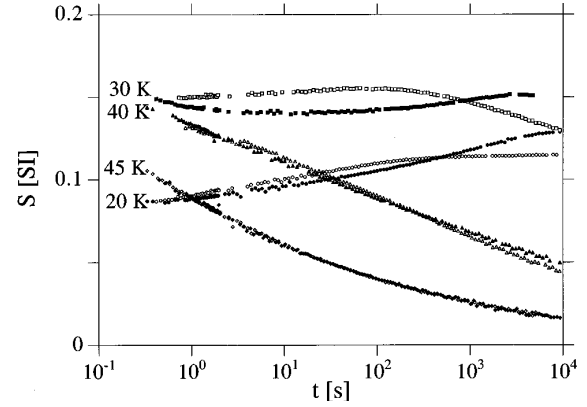


FIG. 3. Relaxation rate S vs observation time at the temperatures 20 K, 30 K, 40 K, and 45 K for the interacting γ - Fe_2O_3 sample. The waiting time t_w at constant temperature before applying the probe field was 10^2 s (open symbols) and 10^4 s (solid symbols).

B. ac susceptibility results

In Fig. 2, χ' and χ'' are plotted vs temperature for the interacting sample and, for a comparison, the noninteracting sample⁸ for the frequencies 15 Hz, 125 Hz, 1 kHz, and 10 kHz. The out-of-phase component for the noninteracting sample has been calculated analytically using the previously determined energy barrier distribution.⁸ It has been shown that the calculated results reproduce the corresponding experimental results to a high degree of precision.⁸ Several differences between the interacting and noninteracting samples can be observed from this figure. In accordance with observations made by others,^{11–17} the maxima of the in-phase component and the corresponding inflection points of the out-of-phase component of the ac susceptibility are shifted towards higher temperatures for the interacting sample. The frequency dependence of χ'' , at constant temperature, is at low temperatures weaker for the interacting sample than for the noninteracting sample, while at high temperatures it appears that the frequency dependence for the interacting and noninteracting samples gradually approach each other. The observation of an almost frequency independent out-of-phase component at low temperatures is in accordance with the observation of a $1/\omega$ dependence in the magnetic noise power spectra at low temperatures. This behavior is similar to the behavior observed in spin glasses well below the spin glass temperature. It is worth noting though that the onset of dissipation, as mirrored by the out-of-phase component of the ac susceptibility, is much more abrupt in a spin glass as compared to the behavior displayed in Fig. 2.

C. ZFC relaxation results

The relaxation rate $S(t_{\text{obs}})$ is shown in Fig. 3 for the temperatures 20 K, 30 K, 40 K, and 45 K. At each temperature, the time dependence of the ZFC magnetization has been measured using two different waiting times $t_w=10^2$ s (open symbols) and $t_w=10^4$ s (solid symbols). At temperatures below 40 K, a clear waiting time dependence of the relaxation rate can be observed. For higher temperatures, a waiting time dependence cannot be resolved in the experimental time win-

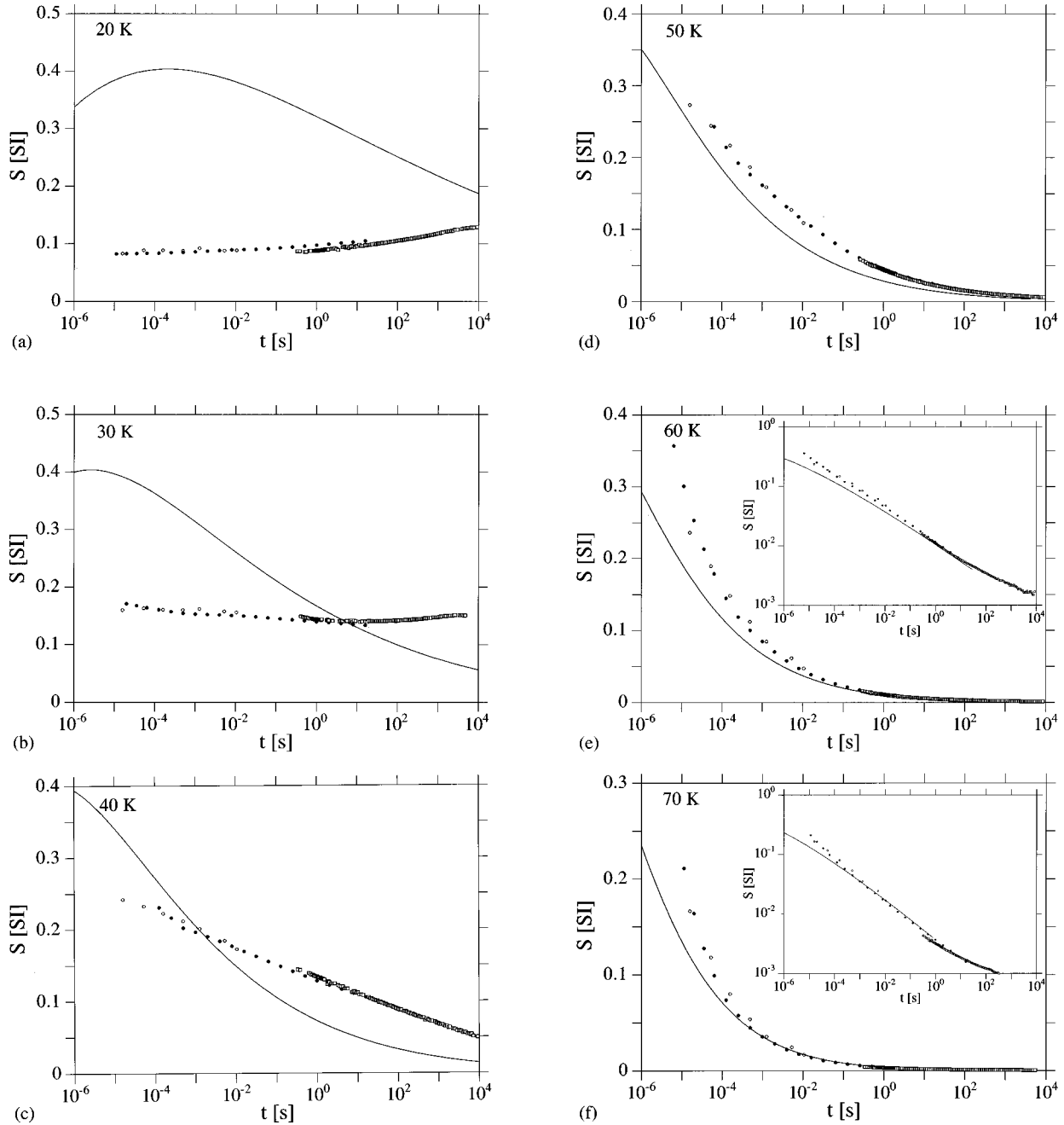


FIG. 4. ac-susceptibility (open circles), magnetic noise (solid circles), and ZFC relaxation (open squares) results plotted as relaxation rate vs observation time at the temperatures (a) 20 K, (b) 30 K, (c) 40 K, (d) 50 K, (e) 60 K, and (f) 70 K. The solid lines correspond to the calculated relaxation rate of the noninteracting sample. In the insets, the same data are shown in semilogarithmic plots. The waiting time in the ZFC relaxation measurements was $t_w = 10^4$ s.

dow. This behavior is in some ways very similar to the behavior of spin glasses and will be discussed in more detail in Sec. IV.

There are also differences between the relaxation behavior of the interacting magnetic particle system and that of spin glasses. Maybe the most obvious difference is that in spin glasses at temperatures above the spin glass temperature, there exists a well-defined temperature-dependent exponential cutoff in the magnetic relaxation where the relaxation rate suddenly drops to zero.²⁷ As can be seen in Fig. 3, the relaxation rate at high temperatures for the nanosized magnetic particle system shows a more gradual approach towards zero.

D. Comparison with the results of the noninteracting sample

In order to cover as wide a time window as possible of the magnetic relaxation of the interacting magnetic particle system, the results from the three different experimental methods have been plotted together as relaxation rate vs observation time in Figs. 4(a)–4(f) for temperatures ranging from 20 K to 70 K. The $P(\omega)$ and $\chi''(\omega)$ data were transformed to relaxation rate using Eqs. (1) and (2), respectively. The plotted results for the ZFC relaxation correspond to the waiting time $t_w = 10^4$ s. By combining these different results, it is possible to cover nine decades in time of the magnetic relaxation. Also displayed in the same figures are the relaxation rates for the noninteracting sample, which have been calcu-

lated using the previously determined energy barrier distribution.⁸

IV. DISCUSSION

The analysis of the results is divided into a low- and a high-temperature region. In the low-temperature region the dynamics is dominated by correlation effects between the particle magnetic moments introducing a SG-like behavior of the magnetic relaxation. In the high-temperature region the magnetic relaxation is instead governed by the dynamics of individual magnetic particles, whose energy barriers are perturbed by dipole fields originating from superparamagnetic particles in the immediate surrounding of the relaxing particles.

In the discussion below, the terms blocked, relaxing, and superparamagnetic particle moments are used. These denominations are defined from the relaxation times of the individual particle moments (τ) according to the conditions $\tau \gg t_{\text{obs}}$, $\tau \approx t_{\text{obs}}$, and $\tau \ll t_{\text{obs}}$, respectively.

A. Low-temperature region

In Fig. 4(a), the relaxation rates at $T = 20$ K are shown for the interacting and the noninteracting samples. In the investigated observation time window, the magnitude of the relaxation rate is considerably smaller for the concentrated sample as compared to the relaxation rate of the dilute sample. This implies, with the assumption that the equilibrium susceptibility is of the same order of magnitude for both samples, that the relaxation rate for the interacting sample will be significantly larger than for the noninteracting sample in the long-time limit. This conclusion is corroborated by the results shown in Figs. 4(b) and 4(c), where the relaxation rates at $T = 30$ K and $T = 40$ K are displayed. At these temperatures, it is seen that dipole-dipole interaction extends the relaxation towards longer times while at the same time it suppresses the relaxation rate at short observation times: i.e., the distribution of relaxation times is broadened and the magnetic relaxation is significantly different from that of the noninteracting sample. The result observed in the low-temperature region is at variance with the predictions of the model proposed by Dormann *et al.*⁹ In this model, the energy barriers are obtained from a set of independent two-level systems. The effect of interparticle interactions, at any temperature, is to increase the average energy barrier and to make the distribution of energy barriers more narrow.²⁶ One consequence of such a model is that the general shape of the relaxation rate curve is preserved; at one given temperature the most noticeable difference in the relaxation rate curve is a shift towards longer time scales. According to the here observed results, the relaxation time spectrum broadens dramatically at low temperatures and it is therefore more appropriate to compare the relaxation of an interacting magnetic particle system with that of frustrated magnetic systems such as spin glasses,^{1,27,28} using a model with a multivalley energy landscape describing the energy barriers of the collective particle state. For a SG below the phase transition temperature the magnetic relaxation extends over all experimentally accessible time scales and the relaxation rate is weakly frequency dependent. This together with the aging property (see below)

suggests that spin-glass-like dynamics should be considered when interpreting low-temperature relaxation results of interacting nanoparticle systems. It should also be pointed out that similar results as those obtained here, when it concerns the effects of interaction on the magnetic relaxation, have been obtained in a recent computer simulation study using a model system consisting of monodisperse magnetic particles with a volume concentration of $\epsilon = 7\%$,²⁰ which shows that a collective particle state must be included at low temperatures (typically for $T < E_{d-d,av}$) to successfully model the magnetic relaxation. The current experimental results and the computer simulation results together present conclusive evidence that a model only considering the modification of the individual particle energy barriers by an interaction field is insufficient to capture the characteristic low-temperature dynamic properties of interacting particle systems.

A striking property of the relaxation in the low-temperature region is the aging behavior. At temperatures below 45 K (cf. Fig. 3), the relaxation rate clearly depends on the waiting time before applying the probe field. The aging phenomenon, mostly known as a feature observed in disordered and frustrated magnetic systems such as spin glasses,^{1,27,28} is a consequence of the chaotic nature of the magnetic state at low temperatures.²⁹ The term chaotic means that only a small perturbation, for instance, a small change in temperature, is able to change the statistical weights of the spin configurations completely. Referring to the droplet model²⁸ the equilibration process can proceed at constant temperature by the growth of a characteristic length scale $R(t)$, describing the average size of regions of correlated particle magnetic moments. Due to the randomness of the magnetic state, the growth of $R(t)$ is logarithmically slow in time.²⁸ If after having equilibrated the particle system for a time t_w the sample is probed by applying a weak magnetic field, the magnetic state of the spin system will as long as the observation time is much shorter than the waiting time, $\ln(t_{\text{obs}}) \ll \ln(t_w)$, be probed at a length scale $L(t_{\text{obs}}) \ll R(t_w + t_{\text{obs}})$, implying that quasiequilibrium dynamics is measured. A crossover to nonequilibrium dynamics is expected at $\ln(t_{\text{obs}}) \approx \ln(t_w)$ since in this case both length scales evolve logarithmically with the observation time, $L(t_{\text{obs}}) \approx R(t_w + t_{\text{obs}})$. Similarly to what is observed for spin glasses the crossover is seen in Figs. 4(a)–4(c) as a distinct change in the relaxation rate. In this study where noise and ac-susceptibility measurements, both reflecting the quasiequilibrium response, are analyzed together with ZFC experiments, it is desirable to use as large waiting time as possible in order to minimize the nonequilibrium effects in the experimental time window.

Above the spin glass temperature T_g it is possible to relate the equilibrium spin-spin correlation length ξ to a relaxation time τ through the relation

$$\tau = \xi^z \alpha (T - T_g)^{-z\nu}, \quad (3)$$

where ν is the correlation length exponent describing the divergence of ξ as T_g is approached from above and z is a dynamic critical exponent. Since neither R nor L can be larger than the equilibrium spin-spin correlation length, magnetic relaxation as well as magnetic aging exist up to time scales of the order τ . Below the spin glass temperature, the

spin-spin correlation extends to very long length scales and magnetic relaxation as well as magnetic aging exists on all time scales in a typical ZFC relaxation experiment.

One important difference between spin glasses and a magnetic particle system is that in a spin glass material all atomic moments are dynamically active, whereas some of the particles in a magnetic particle system may be blocked in the experimental time window. These particles act as temporary random fields as long as they are blocked but change to become a part of the dynamically active particles at long enough time scales. For the low-temperature results, presented in Figs. 4(a)–4(c), it is observed that the relaxation rate for the interacting sample significantly differs from the relaxation rate of the noninteracting sample. This together with the observed aging behavior implies that correlated regions of particles form at low temperatures even in the presence of the random fields created by blocked particles. Moreover, sufficiently close to a possible spin glass transition temperature, the characteristic relaxation time associated with the collective dynamics should exceed all possible time scales associated with the individual particles. At these large time scales, the dynamics becomes governed by a spin glass fixed point and a scaling analysis according to Eq. (3) may be performed. For the here investigated sample, the relatively large width of the volume distribution makes it difficult to experimentally reach the time scales where all particles are dynamically active and hence it is not possible to tell from the results presented in Fig. 3 and Figs. 4(a)–4(c) whether or not also this system exhibits critical behavior. In a recent study, though, using a particle system consisting of nearly monodispersed amorphous FeC particles, it has been shown that critical dynamics according to Eq. (3) indeed can be observed in an interacting particle system.¹⁷ Due to the narrowness of the volume distribution of the FeC particle system, the characteristic time scale associated with collective dynamics exceeds the single-particle relaxation times in the experimental time window.

Comparing now to higher temperatures, it is seen that the aging behavior disappears in the experimental time window (cf. Fig. 3), while the slow magnetic relaxation remains. Moreover, it is seen from Fig. 2(b) that with increasing temperature $\chi''(T)$ of the interacting sample gradually approaches the out-of-phase component of the noninteracting sample. One may therefore hypothesize that at such large temperatures and in the investigated time window, the magnetic relaxation is best described using a single-particle relaxation model. This can be understood as follows. At high temperatures $T > 45$ K, the correlation length describing the size of dynamically correlated particles is comparably small, implying that collective dynamics is only expected to be observed at short time scales. Moreover, in this temperature range the density of relaxing particles is an almost exponentially decreasing function of the logarithm of observation time (particle volume),⁸ implying that the relaxation observed at long time scales is due to a low density of large particles. A low density of such particles implies a larger distance between relaxing particles and hence a comparably small interparticle interaction energy and the relaxation may therefore be described using single-particle dynamics. The relaxation of these comparably large particles may still, however, be influenced by an interaction field originating from

the superparamagnetic surrounding and possibly also from a few even larger blocked particle magnetic moments. It may also be noted that the influence of this ‘‘tail’’ in the relaxation, which may obscure the characteristic relaxation time of the collective dynamics, will decrease with decreasing width of the particle size distribution.

The difference between a magnetic particle system and a spin glass is obvious—in spin glasses slow magnetic relaxation will exist only at low temperatures where the spin-spin correlation length is large while in a magnetic particle system slow magnetic relaxation may, even in the absence of collective dynamics, exist at high temperatures due to the relaxation of a comparably few large particles.

B. High-temperature region

In the high-temperature region, where there is no experimental evidence of collective magnetic relaxation, slow magnetic relaxation is still remaining. According to Figs. 4(d) and 4(e), the magnetic relaxation for the interacting particles sample extends to longer time scales as compared to the case of the noninteracting sample. This suggests that the energy barrier that the magnetic moment of a relaxing particle has to surmount in order to change its direction is perturbed in such a way that the magnetic moment sees a larger energy barrier. The difference in relaxation rate between the interacting and the noninteracting samples decreases with increasing temperature. This behavior is here proposed to arise from the superparamagnetic particles in the immediate surrounding of the relaxing particles.

For the noninteracting sample, a temperature of 45 K corresponds to a probed energy barrier of the order of 10^3 K in the experimental time window of the ZFC measurements. Comparing with the previously extracted energy barrier distribution for these particles,⁸ this implies that 95% by volume of particles give a superparamagnetic response. Even if the energy barriers of the particles in the interacting sample are disturbed by an interaction field, this gives a hint about how large a part of the particle system is in a superparamagnetic state at these temperatures. In the simplest possible model, reminiscent of the model proposed in Ref. 9, it is assumed that in the close surrounding of a relaxing magnetic particle the superparamagnetic particles are polarized by the dipole field due to the larger relaxing particle. The polarized surrounding will in turn create a field (H_p) at the site of the relaxing particle having a direction approximately in parallel with the direction of the magnetic moment of this particle. The consequence of such a field can be evaluated by considering the potential energy for a uniaxial single-domain magnetic particle in the field H_p ,

$$E = KV \sin^2(\theta) - \mu_0 M_s V H_p \cos(\psi), \quad (4)$$

where θ is the angle between the easy direction of magnetization and the magnetization vector and ψ is the angle between the field direction and the magnetization vector. In the case of the magnetic field due to the superparamagnetic surrounding pointing either along or in a direction opposite to the direction of the particle magnetization, the angles can be set equal $\psi = \theta$. The transition rates from one energy mini-

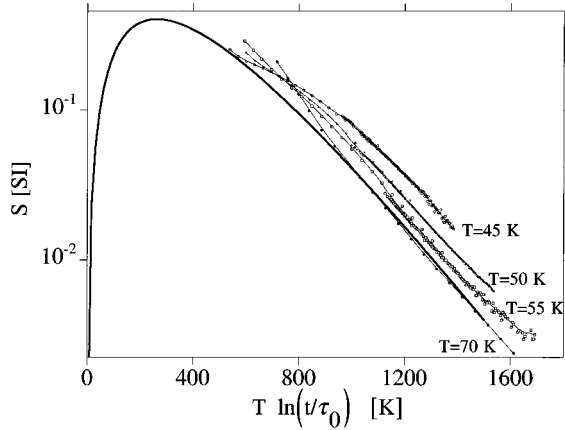


FIG. 5. Relaxation rate data, obtained from magnetic noise and ZFC relaxation measurements at the temperatures 45 K, 50 K, 55 K, and 70 K, plotted vs $T \times \ln(t_{\text{obs}}/\tau_0)$. The thick solid line corresponds to S vs $T \times \ln(t_{\text{obs}}/\tau_0)$ for the noninteracting particle system.

imum to the other depend on the energy barrier seen by the magnetic moment in the following way:³⁻⁵

$$\tau_{\pm}^{-1} = \tau_0^{-1} \exp\left(\frac{-KV(1 \pm h_p)^2}{k_B T}\right), \quad (5)$$

where $h_p = \mu_0 M_s H_p / 2K$ and τ_+ (τ_-) corresponds to the field being parallel (antiparallel) to the magnetization vector. A reasonable assumption is that the reorientation time of the field due to the polarized surrounding is longer than the time needed for the reversal of the particle magnetic moment but considerably shorter than τ_- . In other words, the field due to the polarized surrounding can be considered as constant during the reversal of the relaxing magnetic moment, but will change its orientation according to the new condition set by the field from the switched particle magnetic moment. Thus, the only transition rate which remains important is τ_+^{-1} , which implies that the relaxation time according to Eq. (5) can be written as

$$\tau = \tau_0 \exp\left(\frac{KV(1 + h_p)^2}{k_B T}\right). \quad (6)$$

The effect of the field due to the polarized surrounding is thus to increase the relaxation times of the individual particles. In Fig. 5, the logarithms of the relaxation rates for the temperatures 45 K, 50 K, 55 K, and 70 K are plotted vs $T \times \ln(t_{\text{obs}}/\tau_0)$ together with the relaxation rates for the noninteracting particles. It can be shown that such a plot, in the case of a noninteracting particle system, mirrors the distribution of energy barriers.⁸ The description including a small perturbation field that increases the effective energy barrier is supported by the similar appearances of the relaxation rates of the interacting and non-interacting samples. Except for the lowest temperature shown in Fig. 5, basically a shift of the relaxation rate curves of the interacting sample towards longer time scales is observed. The difference between the relaxation rate curves of the interacting and the noninteracting samples decreases, however, with increasing tempera-

ture. At $T=45$ K, the relaxation rate at short observation times is slightly suppressed, which suggests a crossover from collective behavior to single-particle dynamics occurring in the experimental time window. This is also in agreement with the ZFC aging results, where a waiting time dependence cannot be resolved at experimental time scales and at temperatures $T \geq 45$ K.

It is difficult to construct an accurate model for h_p , but by comparing the results of the interacting and noninteracting particle systems [cf. Fig. 5 and Fig. 2(b)], it is clear that temperature is an important parameter. With increasing temperature the effect of the polarized surrounding decreases which seems reasonable for a collection of superparamagnetic particles with a magnetic state following the Langevin function. Other effects to account for are the volumes of the relaxing particles as well as the number of superparamagnetic particles surrounding each relaxing particle. One thus has to consider the actual shape of the volume distribution of particles, which implies that also the time scale of the experiment becomes an important parameter. Moreover, it is quite likely that quasistatic fields, originating from even larger blocked particles, will contribute and distort the simple picture of only having a field due to the polarized surrounding pointing in the same direction as the direction of the relaxing particle magnetic moment. It is worth noting that the effect of a quasistatic field will be to decrease the relaxation time of the relaxing particles. Provided that such fields exist, it is possible to envisage that at sufficiently high temperatures the relaxation times of the interacting sample will be smaller than the relaxation times of the noninteracting sample. That this can be the case for the present nanoparticle system is supported by Mössbauer results obtained on samples from the same batch of ferrofluid as used in the present work, which clearly show that the characteristic relaxation time of the interacting sample at high temperatures is smaller than for the noninteracting sample.³⁰ These results give evidence that at temperatures $T > 100$ K, the effect of interparticle interactions is reversed. Another model, capable of explaining the Mössbauer results, was proposed in Ref. 10. In this model, which was developed for high temperatures, the interaction field due to the superparamagnetic surrounding is allowed to fluctuate both in size and in direction. The latter assumption leads to a decrease of the relaxation time as the interaction strength increases, thereby giving an explanation for the high-temperature results.

V. CONCLUSION

It has been shown that the magnetic relaxation of an interacting nanosized magnetic particle system at low temperatures is extended towards longer time scales as compared to the relaxation of a noninteracting particle system. Although a considerable part of the particles are blocked at these low temperatures, the magnetic relaxation shows the distinctive mark of collective particle dynamics as evidenced by the chaotic character of the magnetic state of the particle system leading to the observation of magnetic aging. At temperatures higher than 45 K the magnetic relaxation is best described using a model based on single-particle dynamics. Still, there exists an interaction between relaxing magnetic

particles and their immediate surroundings—a relaxing particle will experience a magnetic field due to neighboring superparamagnetic particles and possibly also due to a few large blocked magnetic particles.

ACKNOWLEDGMENT

Financial support from the Swedish Natural Science Research Council (NFR) is gratefully acknowledged.

-
- ¹See, e.g., K. Binder and A. P. Young, *Rev. Mod. Phys.* **58**, 801 (1986).
- ²See, e.g., T. Nattermann and J. Villain, *Phase Transit.* **11**, 5 (1988); D. P. Belanger and A. P. Young, *J. Magn. Magn. Mater.* **100**, 272 (1991).
- ³L. Néel, *Ann. Geophys.* **5**, 99 (1949); W. F. Brown, Jr., *Phys. Rev.* **130**, 1677 (1963).
- ⁴H. Pfeiffer, *Phys. Status Solidi A* **118**, 295 (1990); **122**, 377 (1990).
- ⁵W. T. Coffey, D. S. F. Crothers, J. L. Dormann, L. J. Geoghegan, Yu. P. Kalmykov, J. T. Waldron, and A. W. Wickstead, *Phys. Rev. B* **52**, 15 951 (1995).
- ⁶A. Labarta, O. Iglesias, Ll. Balcells, and F. Badia, *Phys. Rev. B* **48**, 10 240 (1993).
- ⁷H. D. Williams, K. O'Grady, M. El Hilo, and R. W. Chantrell, *J. Magn. Magn. Mater.* **122**, 129 (1993).
- ⁸T. Jonsson, J. Mattsson, P. Nordblad, and P. Svedlindh, *J. Magn. Magn. Mater.* **168**, 269 (1997); P. Svedlindh, T. Jonsson, and J. L. Garcia-Palacios, *ibid.* **169**, 323 (1997).
- ⁹J. L. Dormann, L. Bessais, and D. Fiorani, *J. Phys. C* **21**, 2015 (1988).
- ¹⁰S. Mørup and E. Tronc, *Phys. Rev. Lett.* **72**, 3278 (1994).
- ¹¹J. Zhang, C. Boyd, and W. Luo, *Phys. Rev. Lett.* **77**, 390 (1996).
- ¹²M. El-Hilo, K. O'Grady, and R. W. Chantrell, *J. Magn. Magn. Mater.* **114**, 295 (1992).
- ¹³W. Luo, S. R. Nagel, T. F. Rosenbaum, and R. E. Rosensweig, *Phys. Rev. Lett.* **67**, 2721 (1991).
- ¹⁴K. O'Grady, M. El-Hilo, and R. W. Chantrell, *IEEE Trans. Magn.* **29**, 2608 (1993).
- ¹⁵T. Jonsson, J. Mattsson, C. Djurberg, F. A. Khan, P. Nordblad, and P. Svedlindh, *Phys. Rev. Lett.* **75**, 4138 (1995).
- ¹⁶E. Vincent, Y. Yuan, J. Hammann, H. Hurdequint, and F. Guevara, *J. Magn. Magn. Mater.* **161**, 209 (1996).
- ¹⁷C. Djurberg, P. Svedlindh, P. Nordblad, M. F. Hansen, F. Bødker, and S. Mørup, *Phys. Rev. Lett.* (to be published).
- ¹⁸M. A. Zaluska-Kotur and M. Cieplak, *Europhys. Lett.* **23**, 85 (1993).
- ¹⁹R. W. Chantrell, G. N. Coverdale, M. El. Hilo, and K. O'Grady, *J. Magn. Magn. Mater.* **157**, 250 (1996).
- ²⁰J.-O. Andersson, C. Djurberg, T. Jonsson, P. Svedlindh, and P. Nordblad, *Phys. Rev. B* **56**, 13 983 (1997).
- ²¹Lake Shore, 575 McCorkle Boulevard, Westerville, OH 43082-8888.
- ²²J. Magnusson, C. Djurberg, P. Granberg, and P. Nordblad, *Rev. Sci. Instrum.* (to be published).
- ²³R. Kubo, *Rep. Prog. Phys.* **29**, 255 (1966).
- ²⁴L. Lundgren, P. Svedlindh, and O. Beckman, *J. Magn. Magn. Mater.* **25**, 33 (1981); *Phys. Rev. B* **26**, 3990 (1982).
- ²⁵M. Alba, J. Hammann, M. Ocio, P. Refregier, and H. Bouchiat, *J. Appl. Phys.* **61**, 3683 (1987).
- ²⁶J. L. Dormann, D. Fiorani, and E. Tronc, in *Advances in Chemical Physics*, edited by I. Prigogine and Stuart A. Rice (Wiley, New York, 1997), Vol. XCIII.
- ²⁷P. Svedlindh, P. Granberg, P. Nordblad, L. Lundgren, and H. S. Chen, *Phys. Rev. B* **35**, 268 (1987).
- ²⁸D. S. Fisher and D. A. Huse, *Phys. Rev. B* **38**, 386 (1988); **38**, 373 (1988).
- ²⁹A. J. Bray and M. A. Moore, *J. Phys. C* **17**, L463 (1987).
- ³⁰J. Z. Jiang, S. Mørup, T. Jonsson, and P. Svedlindh, *International Conference on Applications of the Mossbauer Effect, ICAME-95* (Soc. Italiana di Fisica, Bologna, Italy, 1996), Vol. 50, pp. 529–532.